

# Nucleation in Gas-Liquid Transitions

Vicente Talanquer

Department of Chemistry, University of Arizona, Tucson, AZ 85721; vicente@u.arizona.edu

## Background

The dynamic processes that lead to the formation of a new phase in pure fluids and multicomponent mixtures have become a lively area of research in physical chemistry in the past 15 years (1, 2). This burst of attention is driven by the recognition of the central role of the dynamics of phase transitions in atmospheric chemistry, chemical engineering, and material processing. However, few undergraduate chemistry students have the opportunity to develop a clear understanding of what really happens in a system undergoing a phase transition. Conventional curricula in universities and colleges limit most classroom discussions to the analysis of equilibrium phase diagrams and the thermodynamic conditions for phase coexistence. Unfortunately, this knowledge is not enough to explain such fascinating phenomena as the formation of clouds or salt crystals.

Most of the phase transitions that we observe in nature or that are induced during technological processes occur under nonequilibrium conditions. Water at atmospheric pressure, for example, can easily be supercooled below its freezing point of 0 °C without crystallizing. Similarly, most liquids can be superheated tens or hundreds of degrees above their boiling points and gases can be compressed much beyond their equilibrium pressures (supersaturated) before they condense into a liquid (3). In all these cases, a minor perturbation in the system, such as a vibration, a crack on the walls of the container, or the presence of impurities, can trigger the formation of the stable phase. A superheated liquid and a supersaturated gas are examples of what we call “metastable states”, and the range of temperatures and pressures under which these states can be observed depends on factors such as the chemical composition of the system and the characteristics of the container. For pure water at atmospheric pressure, this range extends up to 280 °C for the superheated liquid and down to -41 °C for supercooled states (3).

The existence of metastable states that persist over long periods of time can be explained if we assume that their decay toward the stable phase requires surmounting a free-energy barrier between the metastable state and the stable phase (4). In a supersaturated gas, for example, the phase change is initiated by the formation of density fluctuations in various parts of the system. These fluctuations can be thought of as liquid droplets of different sizes that can act as nuclei for the formation of the new phase. However, small droplets will tend to disappear owing to the high free-energy cost of creating the gas-liquid interface. Only nuclei larger than a critical size will grow, since the energetic advantage of creating a larger volume of the more stable phase overcomes the surface free-energy cost. The time that it takes for the phase transition to occur is determined by the time it takes for these critical nuclei to appear, and this in turn depends on the free-energy cost for their formation. The higher the cost, the longer the lifetime of the metastable state.

Metastable states evolve to a stable phase by nucleation of droplets in supersaturated vapors and superheated crystals, by nucleation of bubbles in superheated liquids, and by nucleation of small crystallites in supercooled liquids. In all these cases, the kinetics of the phase transition is essentially determined by the free energy that needs to be invested to generate a critical nucleus. This “work of formation” defines the height of the free energy barrier that lies between shrinking and growing sections of the stable phase. The size of this barrier depends strongly on temperature and pressure, which explains why different metastable states evolve at different rates. Supercooled water at -2 °C can be kept without crystallizing for several days, whereas ice will appear in seconds at -30 °C. In general, the height of the barrier to nucleation decreases as we move away from the coexistence state.

The process of nucleation of a new phase in the midst of a metastable state has been the subject of diverse experimental and theoretical studies, as well as the center of interest of novel computer simulations (1). This paper presents an overview of some of the most relevant approaches in these areas, with emphasis on the nucleation of fluid phases (liquids and gases). It will illustrate most of the fundamental aspects of nucleation in the particular case of nucleation of a pure liquid from its metastable vapor, and then extend these ideas to other systems of practical interest. Although most of the discussion concerns homogeneous nucleation (5, 6), a brief description of aspects of heterogeneous nucleation involving impurities and surfaces is also presented (3, 4).

## Experiments

To better understand the conditions under which most gas-to-liquid nucleation experiments are carried out, let us first consider a typical pressure-temperature schematic projection of the phase diagram for a pure substance, as that depicted in Figure 1. Lines ab, bc, and bd in this diagram indicate the location of states of two-phase equilibrium. In particular, line  $\overline{bc}$  defines the conditions for liquid-gas coexistence and it ends at the critical point c. If we take a stable gas at a given temperature  $T$  and suddenly increase the pressure over its coexistence value  $P_e$ , the gas phase can persist as a metastable state as long as the pressure does not exceed the limiting value defined by the gas spinodal (dashed line in Fig. 1). Beyond this point, the gas phase is unstable and evolves spontaneously to the liquid state. A metastable gas is said to be “supersaturated” and its supersaturation  $S$  is defined as the ratio of the actual pressure  $P$  of the gas to the coexistence pressure at that temperature:  $S = P/P_e$ . The spinodal line defines the limit of stability for a given phase in a thermodynamic system. In a binary mixture, for example, the spinodal composition defines the maximum supersaturation that can be attained at a given temperature without observing a spontaneous phase separation.

For many years, traditional experiments of nucleation from the vapor were only able to measure the supersaturation  $S$  needed to produce a certain number of growing liquid nuclei per unit time and per unit volume (or rate of nucleation,  $J$ ). For example, in many experiments the critical supersaturation,  $S_{cr}$ , is defined as the supersaturation that leads to a rate of nucleation of  $J_{cr} = 1 \text{ cm}^{-3} \text{ s}^{-1}$  (one droplet per cubic centimeter per second). Note that the lifetime of a metastable state is associated to the inverse of the nucleation rate. During the last 15 years, however, it has become possible to measure actual nucleation rates and use this information to estimate the number of particles that comprise the critical nucleus. Two experimental techniques have been particularly successful in generating reliable results: diffusion chambers and expansion chambers.

The upward thermal diffusion chamber is the most common nucleation instrument (7). It consists of a cylindrical chamber in which a temperature gradient is established between a warm bottom plate and the top of the chamber. The liquid of interest is heated on the bottom plate and diffuses upward through an inert carrier gas whose main function is to help prevent the formation of convection currents in the chamber. The experimental conditions are adjusted to ensure that the gas supersaturation goes through a maximum at about  $\frac{3}{4}$  of the chamber height and to make certain that homogeneous nucleation occurs predominantly at this location. The nucleated droplets grow and fall toward the bottom of the chamber, where a laser beam is used to detect and count the number of falling droplets. This information is then used to calculate the rate of nucleation. Conditions inside the diffusion chamber can be changed to measure nucleation rates as a function of temperature and supersaturation. The instrument is particularly useful under conditions that lead to rates of nucleation in the range from  $10^{-4}$  to  $10^3 \text{ cm}^{-3} \text{ s}^{-1}$ .

In the expansion chamber, nucleation is induced by cooling the vapor by rapid expansion (8). The instrument uses a mixture of the vapor of interest and an inert carrier gas whose main function is to help dissipate the heat generated by the condensation of the liquid. This mixture is expanded adiabatically to a lower temperature at which homogeneous nucleation in the supersaturated vapor occurs. After a short interval of time the pressure is slightly increased in order to halt the nucleation process. The vapor remains supersaturated after the compression to allow the droplets to grow to macroscopic size and then be counted by an optical technique. The existing versions of the expansion chamber have been used to measure nucleation rates in the range from  $10^2$  to  $10^{10} \text{ cm}^{-3} \text{ s}^{-1}$ .

The former experimental techniques have been used to measure the nucleation rates for pure substances such as water,  $n$ -nonane, toluene, and the  $n$ -alcohols, and for binary and ternary mixtures, most of which contain water. The study of the nucleation process in water and in aqueous mixtures is of central interest in atmospheric sciences, where the formation of water droplets and ice crystals has been shown to have a major effect on both short-term and long-term environmental conditions (1, 3). Typical experimental results for the nucleation of water are presented in Figure 2, where we can see that the nucleation rate increases very steeply as a function of the supersaturation at any given temperature.

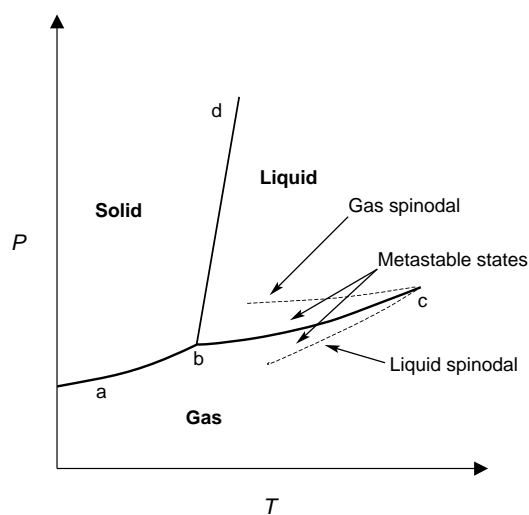


Figure 1. Pressure–temperature phase diagram of a pure substance. The solid lines locate regions of two-phase coexistence (solid–gas, ab; solid–liquid, bd; liquid–gas, bc). The dashed lines indicate the location of the gas and liquid spinodals.

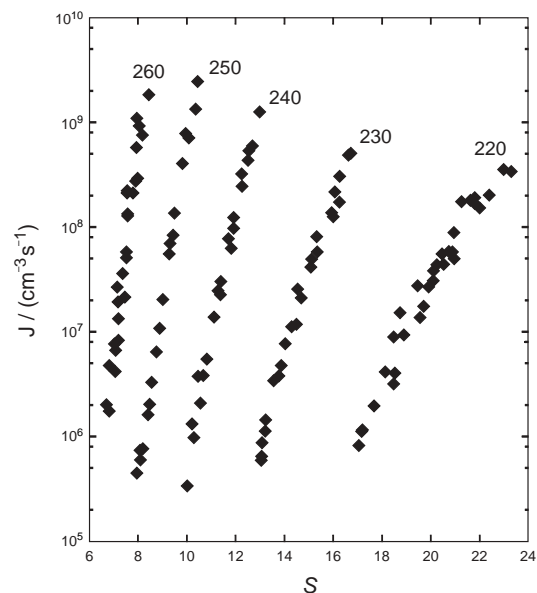


Figure 2. Experimental results for the nucleation rates  $J$  (in droplets per cubic centimeter per second) for the condensation of water as a function of supersaturation  $S$  at different temperatures (in kelvins). Data from ref 27.

## Nucleation Theories

Different theoretical approaches have been developed for the study of nucleation in fluids. Some of them are based on phenomenological theories that predict the properties of the critical nucleus on the basis of the value of macroscopic quantities that are accessible via experimentation. This is the case of the classical nucleation theory (CNT) that has been used for more than 60 years by experimentalists to interpret their results. Other approaches use microscopic models to represent the system's structure and derive its macroscopic

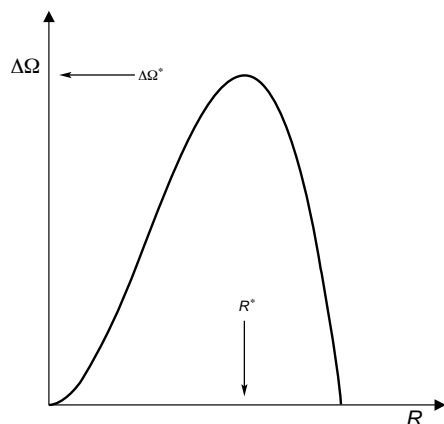


Figure 3. The variation of the free energy  $\Delta\Omega$  required to create a droplet of radius  $R$  according to classical nucleation theory. The critical nucleus corresponds to the droplet with radius  $R^*$  and a maximum work of formation  $\Delta\Omega^*$ .

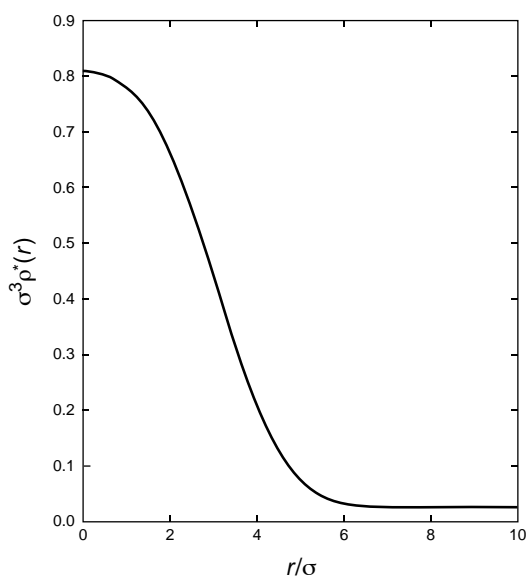


Figure 4. Typical density profile for a critical nucleus  $\rho^*(r)$  in a pure fluid. This function describes the variation of the density as a function of the distance  $r$  to the center of the spherical droplet. The density  $\rho$  and the distance  $r$  are expressed in reduced units of the molecular diameter  $\sigma$  of the particles in the model system (typical values of  $\sigma$  for atoms and small molecules such as Ar and N<sub>2</sub> are in the range from  $2 \times 10^{-10}$  to  $4 \times 10^{-10}$  m).

properties from first principles. That is the case of the density functional theory (DFT) of nucleation. This section will describe the basic ideas behind these two representative theoretical approaches.

#### Classical Theory of Homogeneous Nucleation

In the classical nucleation theory, the work of formation,  $\Delta\Omega$ , of any nucleating droplet in a metastable vapor is estimated by treating it as if it were a small spherical portion of the

bulk liquid (capillarity approximation) (3, 4). The free-energy cost of formation for a droplet of radius  $R$  is thus given by the sum of the gain in free energy associated with the formation of a volume  $\frac{4}{3}\pi R^3$  of the thermodynamically stable phase and the cost of creating a liquid–gas interface of area  $4\pi R^2$ :

$$\Delta\Omega(R) = -\frac{4}{3}\pi R^3 \Delta\omega + 4\pi R^2 \gamma \quad (1)$$

where  $\Delta\omega = \omega_g - \omega_\ell$  is the (positive) bulk free energy difference per unit volume between the metastable and stable phases, and  $\gamma$  is the surface tension of the liquid–gas interface. The free energy difference  $\Delta\omega$  is also a direct measure of the difference between the pressure within the liquid drop and the pressure in the vapor phase,  $\Delta\omega = P_\ell - P_g$ .

The typical behavior of  $\Delta\Omega$  as a function of  $R$  is depicted in Figure 3, where we can see that the function passes through a maximum corresponding to the radius,  $R^*$ , of the critical nucleus. In particular, by taking  $(d\Delta\Omega/dR) = 0$ , we find that

$$R^* = 2\gamma/\Delta\omega \quad (2)$$

(the Laplace equation) and the height of the barrier to nucleation is then given by

$$\Delta\Omega^* = \Delta\Omega(R^*) = 16\pi\gamma^3/(3\Delta\omega^2) \quad (3)$$

According to Figure 3, nuclei with a radius smaller than  $R^*$  will tend to shrink and those with a radius larger than  $R^*$  will tend to grow, since the free energy of the system decreases for any of these processes. The bulk free energy difference  $\Delta\omega$  in eq 3 is a strong function of the pressure and temperature and goes to zero at the thermodynamic conditions at which the two phases coexist. This implies that as coexistence is approached, the size and the work of formation of the critical nucleus diverge, and the lifetime of the corresponding metastable states becomes infinitely long.

The expression for the work of formation in eq 3 can be further simplified by assuming that the nucleating liquid is incompressible. In this case,  $\Delta\omega$  can be expressed as a simple function of the temperature,  $T$ , and the supersaturation,  $S$ ,  $\Delta\omega \approx R_g T \rho_\ell \ln(S)$ , where  $R_g$  is the ideal gas constant and  $\rho_\ell$  is the bulk liquid density (9). The final expression for the work of formation of the critical nucleus in the CNT,  $\Delta\Omega^* = 16\pi\gamma^3/[3(R_g T \rho_\ell \ln S)^2]$ , can then be used to estimate the barrier height to nucleation at any given temperature and supersaturation, since accurate experimental results for  $\gamma$  and  $\rho_\ell$  of most common liquids are readily available.

The rate of nucleation,  $J$ , in CNT is an exponential function of  $\Delta\Omega^*$

$$J = J_0 \exp(-\Delta\Omega^*/RT) \quad (4)$$

where the preexponential factor  $J_0$  depends upon the particular kinetics of cluster formation in the system (5). Because nucleation rates involve exponentials of the barrier to nucleation, they are extraordinarily sensitive to the actual values of the physical properties that determine the value of  $\Delta\Omega^*$ . A small change in the value of the surface tension, for example, can lead to nucleation rates that differ by several orders of magnitude. Thus reproducibility of experimental data can be difficult to achieve. This is why it is surprising that a simple theory such as CNT actually leads to reasonable predictions for the critical supersaturation (value of  $S$  that leads to  $J = 1 \text{ cm}^{-3} \text{ s}^{-1}$ ) for several nonpolar fluids. Unfortunately, the predictions of the classical approach for the actual values of  $J$  in

a wide range of temperatures tend to deviate strongly from the experimental results, predicting too high a rate at high temperatures and too low a rate at low temperatures (1, 2).

One of the central shortcomings of the classical approach to nucleation is the assumption that the properties of any critical nucleus, such as the surface tension and the average internal density, are homogeneous, independent of size, and identical to those of a macroscopic liquid droplet in equilibrium with its vapor. This can hardly be the case for critical nuclei that regularly have sizes from 20 to 50 molecules, as revealed by nucleation experiments for most common fluids. A better theoretical approach would then be to try to derive the properties of the critical nucleus taking into account its microscopic structure. This is the central goal of the density functional theory of nucleation (DFT).

### Density Functional Theory

In the density functional approach, the theoretical work starts by defining a model for the fluid of interest. For example, one can assume that this fluid is composed of hard spherical particles of diameter  $\sigma$  that interact with each other via an attractive potential  $V_{\text{att}}(r_{ij})$  whose strength depends on the distance between particles,  $r_{ij}$ . With our interest in the formation of density fluctuations during the nucleation process, we need to assume that the density of the particles will change from point to point throughout the system. For an inhomogeneous fluid like this, the free energy of the system,  $\Omega$ , depends on the value of the density of particles  $\rho(\mathbf{r})$  at every position  $\mathbf{r}$  throughout the fluid. Thus, we say that  $\Omega[\rho(\mathbf{r})]$  is a "functional" of the density. In a first approximation, the structure of the free energy functional can be expressed as the sum of two main contributions: one purely entropic associated to the different possible configurations of the particles in the fluid, plus an energetic contribution that takes into account the attractive interactions  $V_{\text{att}}(r_{ij})$  between all particles (10):

$$\Omega[\rho(\mathbf{r})] = \int d\mathbf{r} \omega_{\text{hs}}[\rho(\mathbf{r})] + \iint d\mathbf{r} d\mathbf{r}' V_{\text{att}}(r_{ij}) \rho(\mathbf{r}) \rho(\mathbf{r}') \quad (5)$$

In this expression,  $\omega_{\text{hs}}[\rho(\mathbf{r})]$  is the free-energy density of a fluid of hard spheres with local density  $\rho(\mathbf{r})$ , and is essentially a measure of the local entropy in the system.

The minimization of the free energy functional in eq 5 leads to thermodynamic relationships that determine all the thermodynamic properties of the system. These relationships can be used to evaluate the properties of stable and metastable phases at a given temperature and pressure, the structure of the phase diagram, or the surface tension between coexisting phases. They are also useful in determining the function  $\rho^*(\mathbf{r})$  that describes the structure of the critical nucleus sitting at the top of the barrier to nucleation (11, 12). This function outlines the "density profile" of the critical nucleus and can be used, in combination with eq 5, to calculate the work of formation  $\Delta\Omega^*$ . Nucleation rates can then be estimated using the same relationship as that of the classical approach (eq 4).

Figure 4 depicts a typical density profile for a critical nucleus as calculated by DFT. As we can see, its structure is different from that assumed by the classical approach: the density varies continuously from the center of the "droplet" outward, and there is no sharp interface between the liquid and gas phases (the interface between them is diffuse). Moreover, the value of the density at the center of the nucleus decreases with supersaturation and does not necessarily reach the value

of the bulk liquid phase. Only for low values of  $S$ , where critical nuclei are expected to be large, do the properties of the droplets approach those assumed by the classical theory.

In accordance with CNT, the density functional approach predicts that the size of the critical nucleus and its corresponding work of formation diverge at coexistence. However, DFT additionally predicts that  $\Delta\Omega^*$  goes to zero at the spinodal line (11), defined as the location of the thermodynamic states for which the compressibility of the metastable phase goes to infinity. Beyond the spinodal, there is no barrier to nucleation and the new phase appears spontaneously through a dynamic process called spinodal decomposition (3). Most of the deviations between CNT calculations and experimental results for the rates of nucleation of simple fluids are associated with the failure of the classical approach to predict a vanishing work of formation for the critical nucleus at the spinodal.

Theoretical calculations using DFT generate nucleation rates whose dependence on temperature and supersaturation agree qualitatively with experimental results for nonpolar and weakly polar fluids (1, 5). The theory has been particularly useful in understanding the impact of molecular-level effects on the process of nucleation in different types of fluids. Thus, for example, results from DFT indicate that slight changes in the range of the intermolecular interactions between particles can lead to nucleation rates that differ by several orders of magnitude (12) and that the formation of hydrogen bonds in associating fluids increases the barrier to nucleation (13).

Despite the success of different theoretical approaches in explaining and predicting nucleation behavior of pure fluids, there are a wide variety of challenging problems waiting to be solved. In particular, the behavior of strongly polar fluids, such as nitromethane and acetonitrile, is still poorly understood. For these types of systems the actual barrier to nucleation is considerably higher than that predicted using current theoretical approaches (14, 15). It is in the study of more complex systems such as these that computer simulations are providing an attractive alternative.

### Computer Simulations

Computer simulations based on Monte Carlo or molecular dynamics techniques are another example of microscopic approaches that have been used with success to study nucleation processes (1). They offer the possibility of directly determining the position of particles during nucleation events and yield, in essence, exact microscopic information about the model under study. Computer simulations have become increasingly accurate and offer an alternative path to test theoretical predictions, particularly when direct experiments are difficult to perform.

In principle, the most straightforward way to simulate the nucleation of a liquid in a metastable vapor would be to homogeneously distribute a large number of particles in a certain volume in order to generate a supersaturated gas-like configuration, and then use molecular dynamics to solve Newton's equations of motion. The problem with this approach is that current computer simulations can only consider such small volumes ( $10^{-17}$  cm<sup>3</sup>) and short simulation times ( $10^{-8}$  s of real time) that to observe a nucleation event the simulated nucleation rates should be of the order of  $10^{25}$  cm<sup>-3</sup> s<sup>-1</sup>. This number is 15 orders of magnitude larger than the highest

rates that can be measured in a laboratory. To simulate typical experimental rates, the simulation times would have to be increased by a factor of  $10^{20}$ !

Other computer simulation techniques have been devised to study nucleation processes under more realistic conditions. In one of the most common approaches, the properties of an isolated cluster of particles are monitored during the simulation (1). The problem in this case is how to identify those particles that belong to the cluster at any given time (16) and how to keep the cluster intact long enough to determine its average properties. Another alternative has been to force the vapor to nucleate instead of waiting for the spontaneous appearance of the critical fluctuation. This has been accomplished in recent Monte Carlo simulations with the aid of an umbrella sampling technique that assigns a greater statistical weight to configurations of the system that lie between the vapor and the liquid (17). This technique has been applied to simulate the nucleation behavior of a simple model for strongly polar fluids (18). One of the most striking results of this work is that it shows that the symmetry of the critical clusters is not always spherical. In small nuclei composed of up to 30 particles, the dipole moment interactions favor the formation of chain-like clusters. As the cluster size increases, the chain becomes longer, but beyond a certain size the structure collapses into a spherical droplet. However, even for the large spherical droplets, particles tend to arrange in polymer-like structures at the liquid–vapor interface. This peculiar behavior seems to account for the high barrier to nucleation observed in strongly polar fluids and for the failure of theoretical approaches that assume that the critical nuclei for these fluids are spherical and do not exhibit any particular internal structure.

### Three Interesting Problems

#### Cavitation

When a fluid is superheated beyond its boiling temperature, the dynamics of the phase transition are also controlled by the formation of nuclei of the new phase, in this case a stable vapor. During nucleation, small interstitial voids in the liquid coalesce to form a larger cavity or bubble that will grow if its size exceeds a critical value. Similar to the case of gas-to-liquid transition, the work of formation of the critical bubble  $\Delta\Omega^*$  depends on the free-energy cost of its gas–liquid interface and the free energy difference between the stable and metastable phases. The value of  $\Delta\Omega^*$  determines the rate of bubble nucleation (2).

A liquid can also be brought to a metastable state by lowering the external pressure below the liquid's vapor pressure and thus putting it into a state of tension (Fig. 1). All liquids have a measurable tensile strength and under large enough tension they pull apart, generating small bubbles in a process called cavitation. This phenomenon can be induced using a tension pump or ultrasound technology. In the latter case, a longitudinal sound wave causes fluid layers to compress and expand periodically along the wave's direction of propagation. If the amplitude of the acoustic wave is sufficiently large, the total pressure in some regions of the fluid becomes negative and small bubbles (cavities) form (3).

The study of bubble formation in simple fluids using different theoretical approaches reveals that the classical theory of nucleation completely fails to predict reliable cavi-

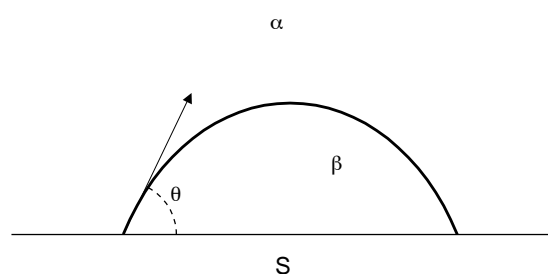


Figure 5. Schematic representation of a droplet on a planar surface;  $\theta$  is the contact angle of phases  $\alpha$  and  $\beta$  with the substrate  $S$ .

tation rates (19). The reason for this is linked to the fact that the spinodal line is much closer to coexistence for the liquid phase, causing the actual height of the barrier to nucleation to decrease much faster than the classical predictions (see Fig. 1). If the predictions of nonclassical approaches such as DFT are correct, liquids exhibit lower tensile strengths than predicted by CNT. However, this is one of the areas in which reliable experimental results are difficult to generate. Liquids are more difficult to purify than gases, and the presence of impurities has a strong impact on measured cavitation rates. Impurities tend to catalyze the formation of bubbles via heterogeneous nucleation.

#### Heterogeneous Nucleation

In the world outside the laboratory, most nucleation is heterogeneous. It is induced on the surface of a foreign body, such as the wall of the container or a small solid particle, or by the presence of a single molecule or ion impurity. The interaction between the fluid particles and the foreign body tends to lower the barrier to nucleation, and critical nuclei form at a much faster pace (20). This is what causes phase transitions in nature to occur close to thermodynamic equilibrium and prevents highly metastable states from forming. In a chemistry lab, we promote the heterogeneous nucleation of bubbles in a heated liquid by adding boiling chips, and thus avoid the formation of a superheated state that can vaporize explosively. The presence of a variety of small particles in the atmosphere, such as sea-salt particles formed by the bursting of air bubbles in breaking waves or aerosol particles generated by industrial combustion or forest fires, induces condensation of water into micro-sized droplets (formation of clouds) at a relative humidity that rarely rises over 101% (3).

Using a classical approach to model the process of nucleation occurring on a solid substrate  $s$ , the critical nucleus may be visualized as a cap-shaped aggregate of the stable phase  $\beta$  surrounded by the metastable phase  $\alpha$  (see Fig. 5). The change in free energy to create a microscopic nucleus of radius  $R$  on the surface is then given by (21):

$$\Delta\Omega = -V\Delta\omega + A_{\alpha\beta}\gamma_{\alpha\beta} + A_{\beta s}(\gamma_{\beta s} - \gamma_{\alpha s}) + \tau L_{\alpha\beta s} \quad (6)$$

where  $V$  is the volume of the nucleus,  $\Delta\omega = \omega_{\alpha} - \omega_{\beta}$  is the bulk free energy difference per unit volume between the metastable and stable phases,  $\gamma_{ij}$  is the interfacial free energy of the corresponding  $ij$  interface of area  $A_{ij}$ , and  $\tau$  is the line tension of the three-phase contact line of length  $L_{\alpha\beta s}$ . The volume  $V$ , areas  $A_{ij}$ , and length  $L_{\alpha\beta s}$  can be expressed as a function of the radius  $R$  and the contact angle  $\theta$  between the

nucleus and the substrate:

$$V = \frac{4}{3}\pi R^3 f(\theta) \quad \text{with} \quad f(\theta) = (2 + \cos \theta)(1 - \cos \theta)^2/4 \quad (7)$$

and

$$A_{\alpha\beta} = 2\pi R^2(1 - \cos \theta), \quad A_{\beta s} = \pi R^2 \sin^2 \theta, \quad L_{\alpha\beta s} = 2\pi R \sin \theta \quad (8)$$

For a given volume  $V$ , the shape that minimizes the work of formation  $\Delta\Omega$  is a spherical sector with the contact angle  $\theta^*$  given by

$$\gamma_{\beta s} - \gamma_{\alpha s} + \gamma_{\alpha\beta} \cos \theta^* + \tau/(R \sin \theta^*) = 0 \quad (9)$$

which reduces to the well-known Young equation,  $\gamma_{\beta s} - \gamma_{\alpha s} + \gamma_{\alpha\beta} \cos \theta_0 = 0$ , in the absence of line tension or when  $R \rightarrow \infty$ . The latter limit corresponds to the case of a macroscopic droplet resting on a planar substrate with an equilibrium contact angle  $\theta_0$ . The critical nucleus that determines the barrier to nucleation has a radius  $R^*$  such that  $\Delta\Omega$  in eq 6 is maximum. By taking  $(d\Delta\Omega/dR) = 0$  and introducing eq 9 into the result, we finally find

$$\Delta\Omega^* = 16\pi\gamma_{\alpha\beta}^3 f(\theta^*)/(3\Delta\omega^2) + 2\pi\tau \sin \theta^* \gamma_{\alpha\beta}/\Delta\omega \quad (10)$$

This expression of the work of formation of the critical nucleus reveals several interesting physical features. Let us examine the case in which  $\alpha$  represents the vapor phase and  $\beta$  the liquid. For systems in which the line tension is not extremely high, the barrier to heterogeneous nucleation for fluids with contact angles smaller than  $180^\circ$  is always smaller than that corresponding to homogeneous nucleation. In fact, for  $\theta^* = 180^\circ$  the droplet detaches from the substrate and the situation returns to one of homogeneous nucleation. On the other hand, in the limit  $\theta^* = 0$ , the liquid wets the substrate and the barrier to nucleation vanishes. This implies that for fluids that wet the surface of their container, the phase transition to the liquid phase will proceed spontaneously in the vicinity of the walls. All these basic results have been confirmed using DFT, which has also revealed the central role that the line tension  $\tau$  plays in determining the height of the barrier to heterogeneous nucleation (21, 22).

Experimental and theoretical research in heterogeneous nucleation of fluids is in its infancy. Few reliable experiments have been performed and less than a handful of computer simulations (23). Nevertheless, the study of the dynamics of phase transitions in porous media is of strong technological relevance, and the phase behavior of fluids inside thin channels has become the center of attention of scientists interested in chemical and biological processes at the level of nanostructures (24). For these more complex systems, it is not only necessary to better understand the influence of the confining walls on the phase transitions, but also to recognize the particular nucleation behavior associated with some multi-component systems.

### Multicomponent Mixtures

Most of the work on nucleation in systems with more than one component has involved binary and some ternary mixtures (1, 2). Comparisons between experimental and theoretical results based on CNT show that the classical approach gives reasonable predictions only for fairly ideal mixtures. For mixtures that exhibit substantial surface enrichment of one of the components, the classical theory can give unphysical

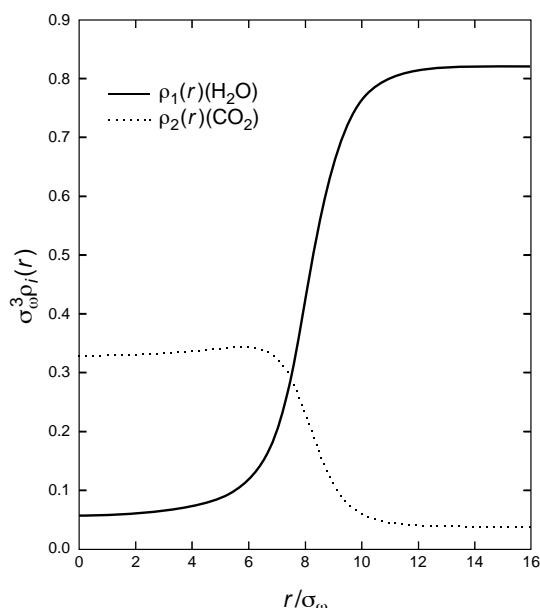


Figure 6. Density profiles of “carbon dioxide” (dashed line) and “water” (solid line) in a critical bubble according to DFT calculations for a simple model of the mixture. The density  $\rho$  and the distance to the center of the bubble  $r$  are expressed in reduced units of the molecular diameter for the “water” molecules  $\sigma_w$  ( $\sim 3 \times 10^{-10}$  m).

results such as a decreasing nucleation rate with an increasing vapor density of the surface active component

The various thermodynamic inconsistencies associated with the classical theory can be avoided by using DFT. This approach has been successfully applied to the study of the formation of droplets and bubbles in binary and ternary mixtures (25). One of the most important results of this work is the confirmation that in systems in which the phase transition is characterized by the variation of more than one independent parameter, such as composition and total density in a binary fluid mixture, the properties of the critical nucleus can differ significantly from those of the stable phase that eventually forms. To illustrate this phenomenon, let us consider the case of mixtures of water and a volatile gas such as carbon dioxide. This type of mixture can be brought into a metastable state by supersaturating the liquid with an excess of dissolved gas. DFT reveals that the critical “bubbles” that initiate the phase separation of the dissolved gas have a high carbon dioxide density and resemble more a liquid droplet than a bubble (see Fig. 6). As the carbon dioxide nucleus grows, its density drops until it becomes an ordinary bubble (26).

This peculiar behavior can be understood if we realize that the interfacial tension for a liquid–liquid interface always tends to be smaller than that for a gas–liquid interface. In the initial stages of nucleation, the work of formation of the smaller nuclei surrounded by water is dominated by the free-energy cost of their interface. Thus the barrier to nucleation will be lower for liquid-like clusters than for gas-like nuclei and the formation of the former will be favored. As the nucleus grows, volume effects will become dominant and the nucleus will gradually adopt the properties of the phase with the lowest bulk free energy (the gas phase in this case). In

general, for multicomponent systems one can expect the smaller nuclei to adopt the structure with the lowest surface free energy. This can favor the formation of nuclei that differ drastically from the bulk stable phase. In a mixture of two partially miscible liquids like methanol and *n*-nonane, in which methanol completely wets the liquid–gas interface, the condensation of *n*-nonane from the vapor mixture will likely be initiated by nuclei that more closely resemble alcohol droplets than alkane clusters.

### Final Remarks

This overview has touched on most of the relevant areas in the study of the process of nucleation in gas–liquid transitions. Its intention is to motivate the introduction of some of the basic ideas of the dynamics of phase transitions to undergraduate courses in physical and atmospheric chemistry and materials science. There is still much to say about nucleation in other types of systems. In particular, the crystallization of pure fluids and multicomponent mixtures is of great interest to physical chemists who have devoted considerable attention to the casting of metals and their alloys, the formation of ionic crystals from solution, the formation of crystallites in glassy materials, and, more recently, the crystallization of proteins from solution (2, 3). Although nucleation in these systems is much less well understood than gas–liquid nucleation, most of the central ideas discussed here still apply. They can be used to develop a basic understanding of processes as diverse as the dewetting of thin liquid films on a surface, the formation of channels in cellular membranes, or the formation of micelles in water–soap mixtures.

### Literature Cited

1. Laaksonen, A.; Talanquer, V.; Oxtoby, D. W. *Annu. Rev. Phys. Chem.* **1995**, *46*, 489–524.
2. Oxtoby, D. W. *Acc. Chem. Res.* **1998**, *31*, 91–97.
3. Debenedetti, P. G. *Metastable Liquids*, Princeton University Press: Princeton, NJ, 1996.
4. Oxtoby, D. W. In *Fundamentals of Inhomogeneous Fluids*, Henderson, D. Ed.; Dekker: New York, 1992; Chapter 10.
5. Oxtoby, D. W. *J. Phys.: Condens. Matter* **1992**, *4*, 7627–7650.
6. Gunton, J. D. H. *J. Stat. Phys.* **1999**, *95*, 903–923.
7. Hung, C.; Krasnopolcer, M. J.; Katz, J. L. *J. Chem. Phys.* **1989**, *90*, 1856–1865.
8. Schmitt, J. L. *Rev. Sci. Instrum.* **1981**, *52*, 1749–1754.
9. Doremus, R. H. *Rates of Phase Transformations*, Academic: New York, 1985.
10. Evans, R. *Adv. Phys.* **1979**, *28*, 143–200.
11. Cahn, J. W.; Hilliard, J. E. *J. Chem. Phys.* **1959**, *31*, 688–699.
12. Oxtoby, D. W.; Evans, R. *J. Chem. Phys.* **1988**, *89*, 7521–7530.
13. Talanquer, V.; Oxtoby, D. W. *J. Chem. Phys.* **2000**, *112*, 851–856.
14. Wright, D.; El-Shall, M. S. *J. Chem. Phys.* **1993**, *98*, 3356–3368.
15. Talanquer, V.; Oxtoby, D. W. *J. Chem. Phys.* **1993**, *99*, 4670–4679.
16. Reiss, H.; Katz, J. L.; Cohen, E. R. *J. Chem. Phys.* **1968**, *48*, 5553–5560.
17. ten Wolde, P. R.; Frenkel, D. *J. Chem. Phys.* **1998**, *109*, 9901–9918.
18. ten Wolde, P. R.; Oxtoby, D. W.; Frenkel, D. *J. Chem. Phys.* **1999**, *111*, 4762–4773.
19. Zeng, X. C.; Oxtoby, D. W. *J. Chem. Phys.* **1991**, *94*, 4472–4478.
20. Turnbull, D. *J. Chem. Phys.* **1959**, *18*, 198–203.
21. Talanquer, V.; Oxtoby, D. W. *J. Chem. Phys.* **1996**, *104*, 1483–1492.
22. Padilla, K.; Talanquer, V. *J. Chem. Phys.* **2001**, *114*, 1319–1325.
23. Yasuoka, K.; Gao, G. T.; Zeng, X. C. *J. Chem. Phys.* **2000**, *112*, 4279.
24. Gelb, L. D.; Gubbins, K. E.; Radhakrishnan, R.; Sliwinka-Bartkowiak, M. *Rep. Prog. Phys.* **1999**, *62*, 1573–1659.
25. Talanquer, V.; Oxtoby, D. W. *J. Chem. Phys.* **1995**, *102*, 2156–2164; **1996**, *104*, 1993–1999; **1997**, *106*, 3673–3680.
26. Talanquer, V.; Cunningham, C.; Oxtoby, D. W. *J. Chem. Phys.* **2001**, *114*, 6759–6762.
27. Viisanen, Y.; Strey, R.; Reiss, H. *J. Chem. Phys.* **1993**, *99*, 4680–4692; Erratum: *J. Chem. Phys.* **2000**, *112*, 8205.